UCID--19692

DE83 008204

A REVIEW OF INTENSE-ION-BEAM PROPAGATION WITH A VIEW TOWARD MEASURING ION ENERGY

Manuel Garcia

Lawrence Livermore National Laboratory
University of California
Livermore, California 94550

25 August 1982

CONTENTS

CONTENTS (Continued)

ABSTRACT

The subject of this review is intense ion beam propagation and the possibilities of measuring time dependent ion energy in the beam. Propagation effects discussed include charge separation, charge and current autoneutralization, electron thermalization and current neutralization decay. The interaction of a plasma beam with material obstacles, like collimators, and with transverse magnetic fields is also described. Depending on beam energy, density and pulse length, these interactions can include material ablation with plasmadynamic flow and undeflected propagation across transverse magnetic fields by a polarization drift. On the basis of this review I conclude that three diagnostics: a single floating potential probe, net current probes (Faraday cups) and a Rutherford scattering spectrometer appear capable of giving prompt, time dependent ion energy measurements.

ACKNOWLEDGMENTS

In India the word guru is understood to mean any person who knowingly or unknowingly enhances your awareness however short the engagement. I am pleased to acknowledge the gurus of my education in beam propagation.

David Kraybill introduced me to this subject and generously allowed me to horde his copy of Plasma Diagnostic Techniques. Ramon Leeper and Tom Lockner of Sandia National Laboratories in Albuquerque were generous with their time, gave me many insights, sustained many questions and gave me wonderful tours of the unique beam fusion facilities they work with. Tom gave me a copy of Reference 4, my introduction to ion beam literature, and Ramon described many

diagnostic techniques, especially the Rutherford scattering spectrometer he is developing. I am grateful to Paul Drake and Mike Campbell for taking time out to listen to my ideas on a floating probe measurement of ion energy and to define the fundamental questions that had to be answered to prove its feasibility. Throughout the entire period that I was developing this report I would buttenhole Jim Morgan, Lloyd Multhauf and Larry Wiley to listen to my latest idea as I was baking it. Gentlemen, I appreciate it. Jim, thank you for References 23 and 26. David Redhead has, on numerous occasions, helped me answer questions about circuits and experimental reality. De Lynn Clark and Mike Moran were both very helpful in describing proton detectors and spectrometers. Finally I must thank Professor Takaya Kawabe and his student Takashi Ikehata in Tsukuba, Japan and Scott Robertson and Hiroshi Ishizuka in Irvine, California for describing their experiments with double floating probes in magnetized plasma beams over the telephone and in clear readable papers. Appendices 4 and 5 are comments by Stanley Humphries Jr. and Tom Lockner to the first edition of this report. Humphries' comments on beam neutralization and the initial probe transient elicited by the arriving beam front are succinct and illuminating. Lockner's comments led me to detect errors in my ion cyclotron radius calculations and re-evaluate magnetic spectrometers.

The crisp figures in this report are the work of Lisa Shaw and Bill Edwards. The masterful transformation of my dense handwritten manuscript into open, presentable text is the work of Elke Jones.

The reader of this report should be aware that the statements and conclusions made as well as any inaccuracies or misrepresentations of the work of others are clearly my own. However, I welcome any opportunity to clarify confusion and add the reader to my list of gurus.

LIST OF SYMBOLS

A_p	floating probe electrode area (cm^2)
A_w	atomic weight (gm/mole)
B	magnetic field (induction) (gauss)
B_c	critical magnetic field for electron magnetic insulation (gauss)
B_L	Lorentz magnetic field: polarization drift (gauss)
C_p	capacitance of floating probe (F)
c	2.99795×10^{10} cm/sec speed of light in vacuo
D	beam diameter at x = 0 (cm)
D_w	drift tube diameter (cm)
d	accelerator and/or magnetically insulated gap (cm)
E	electric field (V/cm), here polarization electric field
E_0	ion rest mass energy (volts)
E_{0e}	electron rest mass energy (volts)
E_K	ion kinetic energy (volts)
E_{Ke}	electron kinetic energy (volts)
e	1.6021×10^{-19} (Joule/eV = coul.)
F_1	inertial reference frame fixed to ion velocity v_+
h_{De}	electron Debye length (cm)
h_{DL}	longitudinal Debye length (cm)
h_{DT}	transverse Debye length (cm)
I_+	beam ion current (amps)
I_e	neutralization electron current (amps)

$I_{+_{th}}$	ion thermal or transverse current (amps)
$I_{e_{th}}$	electron thermal or transverse current (amps)
I_p	floating probe current (amps)
j	net beam current density (amps/cm^2)
j_+	beam ion current density (amps/cm^2)
j_e	beam electron current density (amps/cm^2)
$j_{+_{th}}$	transverse ion current density (amps/cm^2)
$j_{e_{th}}$	transverse electron current density (amps/cm^2)
j_{+0}	j_+ at x = 0
k	1.3807×10^{-23} °K/Joule Boltzmann's constant
L	beam propagation distance (cm)
L_w	drift tube inductance (Henry)
l_+	ion range (cm)
l_α	alpha range (cm)
l_c	net current probe filter thickness (cm)
l_w	drift tube length (cm)
m_+	ion mass (gm)
m_{+0}	m_+ at rest
m_e	electron mass (gm)
m_{e0}	m_e at rest
N	atomic density (atoms/cm^3)
N_0	6.022×10^{23} (gm-mole)$^{-1}$ Avogadro's number
n_+	ion density (cm^{-3})
$n_{+\infty}$	undisturbed or free stream ion density

n_{+0}	n_+ at $x = 0$
n_e	electron density (cm^{-3})
$n_{e\infty}$	undisturbed or free stream electron density
P	beam energy flux ($watts/cm^2$)
P_p	power dissipated in floating probe (watts)
R_p	floating probe impedance (ohms)
r_+	beam radius (cm)
r_{c+}	ion gyroradius (cm)
r_{ce}	electron gyroradius (cm)
T_+	ion temperature in volts
T_+^0	ion temperature in °K
T_e	electron temperature in volts
T_e^0	electron temperature in °K
T_c^0	critical material temperature gain per atom (°K)
t	time (sec.)
t_F	beam flight time in a drift tube (sec.)
t_p	floating potential lag time (sec.)
V_c	negative bias voltage on net current collector probe (volts)
V_F	floating potential (volts) (subscripts 1 and 2 for double probe)
V_s	space potential (volts)
v_+	ion velocity (cm/sec)
v_e	electron velocity (cm/sec)
$v_{+_{th}}$	ion thermal (average) velocity (cm/sec.)
$v_{e_{th}}$	electron thermal (average) velocity (cm/sec.)
$v_{s_{th}}$	species s thermal (average) velocity (cm/sec.)

x	axial distance from accelerator/drift tube interface (cm)
x_s	axial extent for magnetic deflection y (cm)
y	transverse coordinate (radial) (cm)
y_s	lateral deflection in a transverse magnetic field (cm)

* * *

Γ_s	*random thermal particle flux of species s* (cm^{-2} sec^{-1})
Γ_e	electron thermal flux (cm^{-2} sec^{-1})
Γ_+	ion thermal flux (cm^{-2} sec^{-1})
ϵ	permittivity of a plasma (farad/cm)
ϵ_0	8.8542 x 10^{-14} farad/cm permittivity of free space
ϵ_B	*energy per atom delivered by a beam pulse to a material target* (joule/atom)
ϵ_c	critical energy per atom for material breakdown (joule/atom)
$d\theta$	beam divergence half angle in radians
μ	m_e/m_+ mass ratio
μ_0	4Π x 10^{-9} *henry/cm permeability of free space*
ν_{p+}	ion plasma frequency (Hz)
ν_{c+}	ion cyclotron frequency (Hz)
ν_{ce}	electron cyclotron frequency (Hz)
ν_{pe}	electron plasma frequency (Hz)
$\nu_{p_{+0}}$, $\nu_{c_{+0}}$ $\nu_{p_{e0}}$, $\nu_{c_{e0}}$	use rest mass (Hz)
ξ	y/h_{De} scaled transverse coordinate
ρ	density (gm/cm^3)

ρ_{net} space charge

net space charge density = $e(n_+ - n_e)$ (coul./cm^3)

τ characteristic current neutralization decay time (sec.)

τ_c time to reach c_c at given P (sec.)

τ_B beam pulse width (sec.)

τ_{RC} response time of floating probe (sec.)

ω_{p+} ion plasma frequency (radians/sec.)

ω_{pe} electron plasma frequency (radians/sec.)

ω_{c+} ion cyclotron frequency (radians/sec.)

ω_{ce} electron cyclotron frequency (radians/sec.)

$\left.\begin{matrix}\omega_{p_{+0}}, \omega_{c_{+0}} \\ \omega_{p_{e0}}, \omega_{c_{e0}}\end{matrix}\right\}$ use rest mass (radians/sec.)

LIST OF EXAMPLES

1. INTRODUCTION

Work is underway to develop ion accelerators capable of producing megavolt energy kiloampere beams.[1] Applications for these accelerators include beam weaponry, space propulsion and light ion beam inertial confinement fusion. What would an experimenter have to measure to determine directed beam energy? This depends on the ion current density. Any experiment which attempts to measure beam energy must account for the effects of beam propagation between the accelerator and the measurement station. These propagation effects can include neutralization[1,2,3,4] and plasmadynamic flow effects.[5]

Figure 1 illustrates the generic experimental arrangement I will discuss. An accelerator ($x < 0$) produces an ion beam of density n_+ (cm^{-3}), directed energy $E_K = m_+v_+^2/(2e)$ (volts), current density j_+ ($amps/cm^2$) and ion temperature T_+ (volts). The ion temperature is a parameter describing the degree of collimation of the ion beam emitted by the accelerator. An implicit assumption is that $T_+ << E_K$. For $x > 0$ the beam is in a drift tube which is simply an electrically grounded pipe. The interface between the accelerator and the drift tube ($x = 0$) may be an open hole (a collimator) or a thin solid barrier (vacuum barrier). In either case electrons will be introduced into the beam.

Consider a progression of increasing ion current density. For extremely low beam densities, single particle motion may be considered. Single ions propagate through a vacuum without energy loss and are available for analysis by a spectrometer consisting of a bending magnet and detector array. Filters or sweeping magnets are used to prevent stray electrons from impinging the

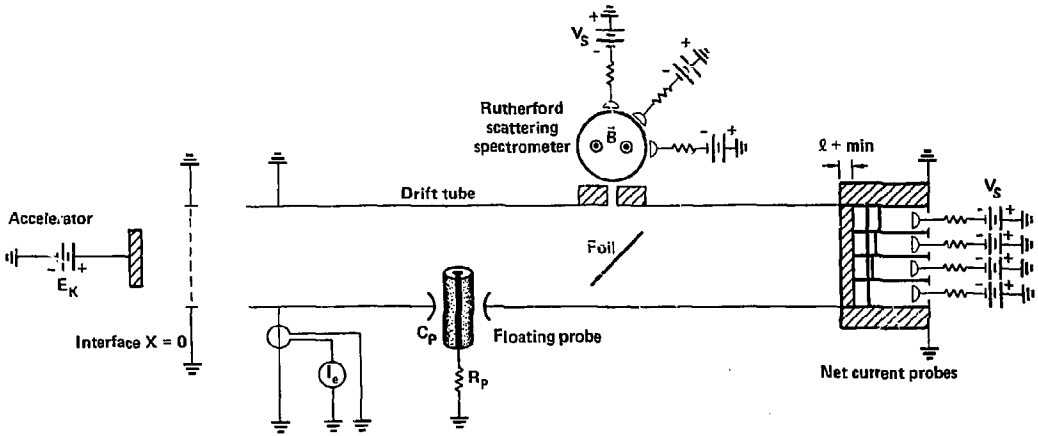

Figure 1. Beam propagation experiments

detectors. Greater ion current density implies stronger signals. As ion current density increases, the effect of ion beam spread due to mutual repulsion becomes apparent.[6] Thus, increasing ion current density at the detector requires progressively larger increases at the accelerator and eventually becomes impossible. As the ion space charge increases, intense electric fields are created which attract electrons from the interface region of the drift tube rapidly neutralizing the beam.[7] Neutralization balances change, $n_e = n_+$, and cancels current $v_e = v_+$. Nature abhors space charge. A high current density, high energy ion beam autoneutializes at the interface and the zero net current plasma beam propagates with negligible spread characterized by T_+. Ions need only surrender the fraction m_e/m_+ ($\leq 1/1836.2$) of their energy to accelerate electrons to ion speed v_+. The neutralization process leaves ion momentum and beam energy essentially unchanged. After a period of time determined by boundary conditions (the drift tube geometry) the current neutralization but not the charge neutralization will disappear ($v_e \rightarrow 0$, $n_+ = n_e$). The ion momentum and energy remain unchanged but the beam will exhibit a net current density j_+; ions will be streaming through a stationary electron cloud.

The exposition of this report follows an ion beam in its flight along a drift tube.

In Section 2 I describe electrical shielding lengths and demonstrate their use as quantitative measures of current density, replacing the adjectives "high" and "low."

In Sections 3 I describe the concept of autoneutralization and show that current neutralized beams will exhibit a space potential V_s above ground which represents the net energy gained by electrons accelerated to ion speed.

In the course of being entrained by the ion flow these electrons thermalize somewhat to a temperature T_e that is significantly less than ion temperature T_+ or either of the kinetic energies E_K and V_s. I also discuss the lifetime of current neutralization and the potential diagnostic value of current neutralization decay.

In Section 4 I describe a floating potential measurement of ion directed energy E_K in a current neutralized beam. The concept of the floating potential V_F and its relationship to space potential V_s as well as electron and ion temperatures T_e and T_+ is described. Using the relationship between V_s and E_K shown in Section 3, the floating potential is related directly to the ion kinetic energy. Experimental experience would seem to indicate that the floating probe described could be built with nanosecond response time.

The interaction of ion beams with material surfaces is discussed in Section 5 in order to estimate the effects of beam collimation. Massive collimation of high current density, multi-keV plasma beams has been shown to drastically alter beam properties downstream.[5] Collimators create regions of stagnated, compressed plasma where directed kinetic energy is redistributed into random energy modes and ablation. The collimator opening is an orifice through which this plasma plenum expands. The downstream plasma beam has been stagnated, thermalized, compositionally altered and re-expanded. The depth of penetration, or range l_+, of multi-MeV ion beams is so much greater than that of multi-keV beams that the beam energy is dissipated in much more material. As a result, ablation and the plasmadynamic flow effects described can usually be avoided in multi-MeV beams.

The effect of transverse magnetic fields on beam propagation are considered in Section 6. The polarization drift is described and a formula given for the minimum magnetic field required to deflect beam ions.

In Section 7 a general survey of diagnostic methods is given and three promising avenues are identified: net current probes, a Rutherford scattering spectrometer and single floating probes.

2. ELECTRICAL SHIELDING LENGTH

Consider an ion beam of n_+ ions/cm^3 accelerated toward positive x to a directed kinetic energy of $E_K = m_+v_+^2/(2e)$ (volts) at x = 0. The ion transverse temperature is $T_+ << E_K$. The gap across which the ions are accelerated will contain n_e electrons/cm^3 (of order n_+) which are prevented from traveling with the ion beam (say by externally imposed transverse magnetic fields) past x = 0. As more ions travel down the drift tube (x > 0), more electron space charge builds up in the accelerator gap and at the interface (x = 0). How much distance can the drift tube ions put between themselves and the electron space charge by expending all of their directed kinetic energy? Dimensionally we would expect:

$$\frac{\text{ion energy}}{(\text{separation})^2} \propto \text{net space charge}$$

$$\frac{E_K}{L_{\text{separation}}^2} = \frac{\rho_{\text{net space charge}}}{\epsilon_0} = \frac{en_+}{\epsilon_0}$$

$$L_{\text{separation}} = h_{DL} = \sqrt{\frac{\epsilon_0 E_K}{en_+}} \quad . \tag{2.1}$$

h_{DL} is a Debye length based on directed ion energy (L = longitudinal) and ion beam density. Charge separation is limited by the available energy to distances of order h_{DL}. On average, charge neutrality obtains for distances greater than h_{DL}. The beam essentially stops, or it attracts electrons, becomes neutralized and propagates as a plasma.[8]

Substituting the ion transverse temperature T_+ (volts) for E_K in (2.1)

$$h_{DT} = \sqrt{\frac{\epsilon_0 T_+}{e n_+}} \qquad (2.2)$$

results in a Debye length based on ion thermal motion or beam divergence. h_{DL} and h_{DT} are the appropriate longitudinal and transverse length scales which characterize the electrical properties of the beam.

Consider the following numerical example of an ion beam:

Example 1.

$n_+ = 5.12 \times 10^{10}$ cm^{-3}, protons

$E_K = 20$ MeV

$j_+ = 50$ amp/cm^2

$T_+ = 18.5$ keV (2° beam 1/2 angle divergence) (see Appendix 1)

$v_+ = .2c = 6.09 \times 10^9$ cm/sec

$v_{+_{th}} = .007c = 2.13 \times 10^8$ cm/sec.

Using the Debye length formula

$$h_D = 743 \sqrt{\frac{\text{energy in volts}}{\text{density in cc}}} \quad cm \qquad (2.3)$$

we arrive at:

$h_{DL} = 14.7$ cm

$h_{DT} = .4$ cm .

In Example 1, 20 MeV of energy must be expended per ion to separate 5.12×10^{10} of them from an equivalent number of electrons a distance of 14.7 cm. This elementary example, and extensive experimental experience,[6] demonstrates that any ion beam that is to propagate a distance $L > h_{DL}$ must be neutralized.

Defining

L = propagation distance from the accelerator-drift tube interface ($x = 0$) to the measurement station.

D = beam diameter at $x = 0$.

I can quantify the terms "one dimensional," "low" and "high current density" beams as follows:

a) one dimensional propagation: $h_{DT} < D$ (2.4a)

b) low current density beam: $h_{DL} > L$ (2.4b)

c) high current density beam: $h_{DL} < L$. (2.4c)

Low current density beams remain unneutralized along their flight path, high current density beams are neutralized as plasma flows. This neutralization process is described in the following section.

3. NEUTRALIZATION

3.1. LONGITUDINAL AUTONEUTRALIZATION

A one dimensional ion beam propelled into an evacuated drift tube through a grounded potential surface at x = 0 will draw electron current out of the infinite supply at ground and become a charge and current neutralized plasma flow by[3,7]

$$x = .5h_{DL} \quad (= 7.4 \text{ cm})^{(9)} \quad . \tag{3.1.1}$$

The ion beam surrenders m_e/m_+ of its directed energy in order to accelerate stationary ($v_e = 0$) ground electrons to the ion velocity v_+. Ion energy is negligibly affected by the neutralization process as

$$\mu \equiv \frac{m_e}{m_+} \leq \frac{1}{1836.2} \quad . \tag{3.1.2}$$

Electrons are accelerated by a net potential rise of

$$V_s = \mu\left(\frac{1}{2} m_+ v_+^2 \frac{1}{e}\right) \qquad (= 10.89 \text{ kV})^{(9)} \tag{3.1.3}$$

across a sheath (a non-neutral charge layer) approximately $.5h_{DL}$ long. As electric fields vanish in neutral plasmas (i.e. over lengths > h_{DL}) the entire neutral flowfield floats up to a space potential of V_s above ground. (See Fig. 2.)

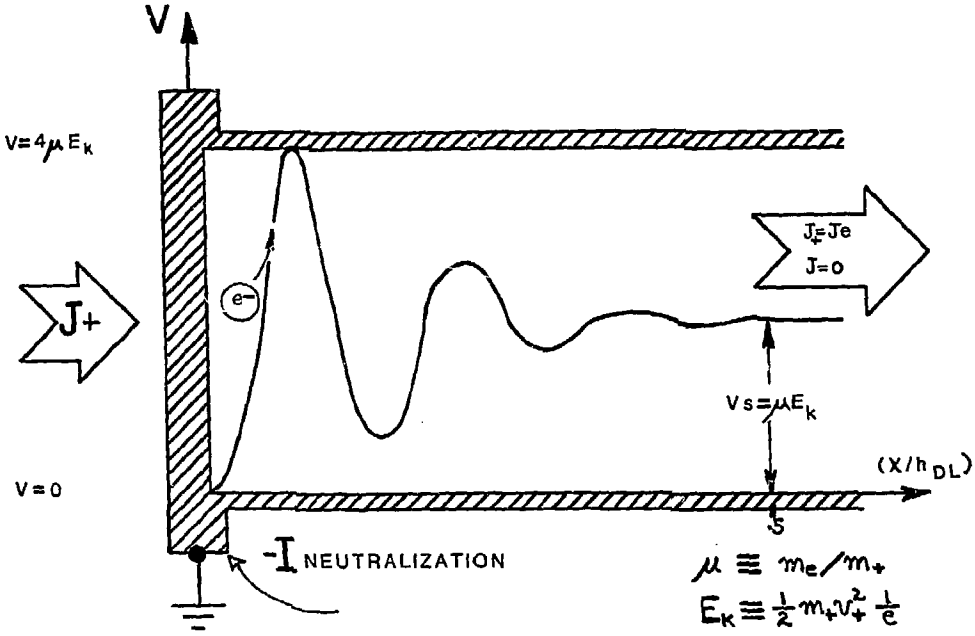

Figure 2: LONGITUDINAL AUTONEUTRALIZATION

3.2. DECAY OF CURRENT NEUTRALIZATION

An autoneutralized beam which spans a closed conducting container ($\tau_B > t_F$), such as a drift tube capped at both ends, will remain charge neutral ($n_e = n_+$) but will lose its current neutralization ($v_e \to 0$). Once an extended stationary electron space charge equal to the ion beam space charge is established inside the chamber, the electron neutralization current stops and a net current density j_+ propagates through. The lifetime of the electron neutralization current (after the beam flight time to traverse the chamber) is limited by the chamber inductance with a characteristic decay time[10]

$$\tau = \frac{I_+ L_w}{\mu E_K} = \frac{I_+ L_w}{V_s} \tag{3.2.1}$$

where

$$I_+ = j_+ \frac{\pi D^2}{4} \tag{3.2.2}$$

$$L_w = \text{inductance of grounded enclosure} \quad . \tag{3.2.3}$$

When the enclosure is a capped pipe with

$$D_w = \text{drift tube diameter } (\geq 2D) \tag{3.2.4}$$

$$l_w = \text{drift tube length} \tag{3.2.5}$$

the inductance is:[10]

$$L_w = \frac{\mu_0 l_w}{4\pi} \ln (D_w/D) \qquad (3.2.6)$$

where $\mu_0 = 4\pi \times 10^{-9}$ henry/cm, the permeability of free space. By 5τ the electron neutralization current has decayed (see Fig. 3).[4]

$$I_e = \frac{-I_+}{1 + t/\tau} \qquad (3.2.7)$$

The beam flight time to traverse the drift tube is

$$t_F = l_w/v_+ \quad . \qquad (3.2.8)$$

The ratio τ/t_F is independent of l_w and found by combining equations, (3.2.1), (3.2.6) and (3.2.3):

$$\frac{\tau}{t_F} = \frac{I_+}{\left(\frac{V_s}{\frac{\mu_0}{4\pi} \ln (D_w/D) \quad v_+}\right)} \quad . \qquad (3.2.9)$$

Clearly

$$\tau \begin{matrix} > \\ = \\ < \end{matrix} t_F \qquad (3.2.10)$$

as

$$I_+ \begin{matrix} > \\ = \\ < \end{matrix} \frac{V_s}{\frac{\mu_0}{4\pi} \ln (D_w/D) \quad v_+} \quad . \qquad (3.2.11)$$

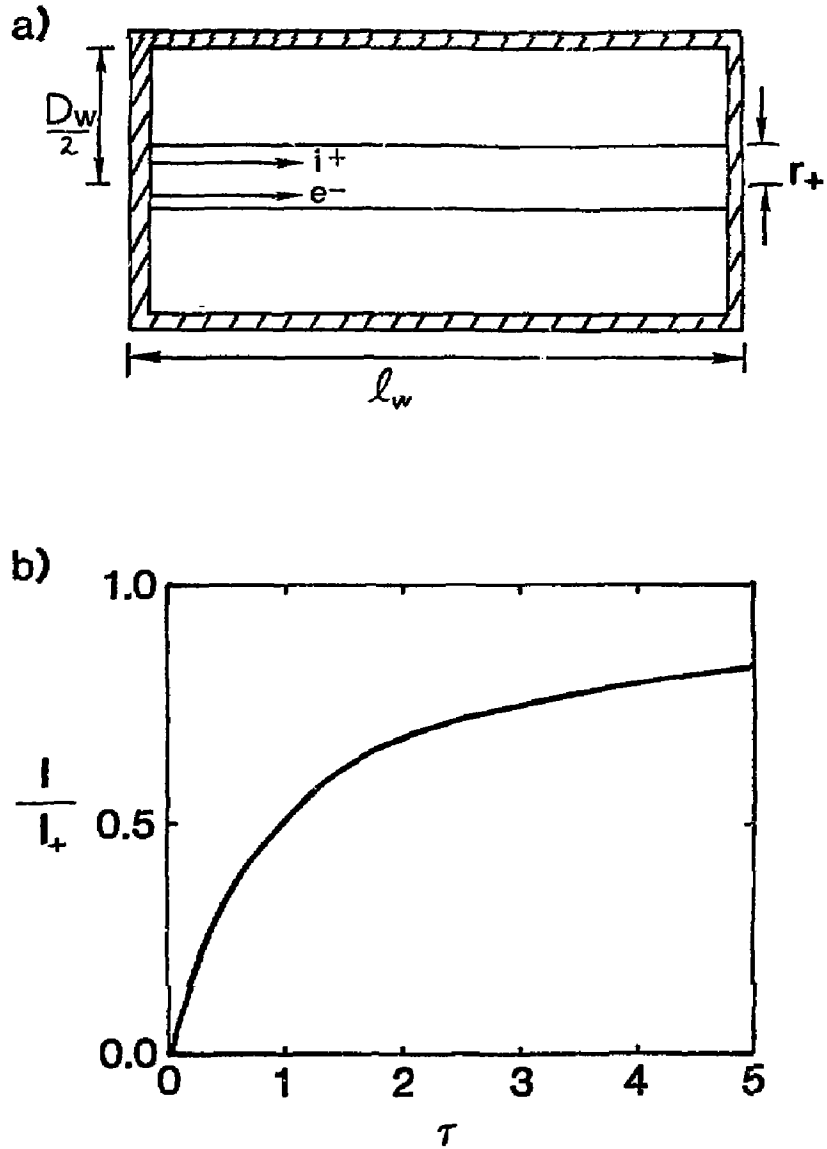

Figure 3. Generation of net currents in auto-neutralizated ion beams moving through regions bounded by conductors. (a) Geometry and parameters of calculation. (b) Normalized growth of net current ($I = I_e + I_+$) with time, where I_e is the neutralizing electron current, I_+ is the ion current, and τ is defined in the text. Solution valid when $r_+ < r_w/2$.

Example 2.

As an example consider the reference 20 MeV 50 A/cm^2 proton beam autoneutralizing in the following drift tube:

$D_w/D = 2$

$l_w = 400$ cm

$L_w = 2.77 \times 10^{-7}$ henry

$I_+ = 1000$ A (a 2" diam beam in a 4" diam pipe)

$t_F = 66$ ns

$\tau = 26$ ns.

For the characteristic neutralization decay time τ to equal the 66 ns flight time the ion current would have to be 2.58 kA or $j_+ = .129$ KA/cm^2. Alternatively the 1000 A proton beam in a drift tube with $D_w/D = 6$ would exhibit $\tau = t_F = 66$ ns. The longer and wider the pipe in which an ion beam propagates, the longer its life as a charge and current neutralized plasma flow.

Let time be referenced ($t = 0$) to the moment the positive ion beam first crosses the interface at $x = 0$ into a closed ended drift tube. For $t < t_F + \tau$, a plasma flow with zero net charge and current, at a space potential $v_s = \mu m_+ v_+^2/(2e)$ above ground and with velocity v_+ can be assumed. For $t > t_F + 5\tau$, a stream of positive current $I_+ = en_+v_+\pi D^2/4$ propagates through an enclosed region of zero net space charge ($n_e = n_+$) at a minimal space potential ($v_e = 0$, $v_{e_{th}} > 0$). The transition between these two regimes takes about 5τ.

One can measure an average ion directed energy by monitoring the decay of the electron neutralization current in a closed, conducting drift tube probe.[11] Combining Eqs. (3.2.1) and (3.2.7) with a measured time history of I_e:

$$|I_e\ (t \leq t_F)| = |I_+\ (t \leq t_F)| \tag{3.2.12}$$

$$\overline{E_K} = \frac{\overline{|I_e\ (t \leq t_F)|}\ L_w}{\mu\ \tau} \tag{3.2.13}$$

where the bar signifies a time average. After I_e decays ($t \geq t_F + 5\tau$) the drift tube probe will simply collect time resolved ion current $I_+(t > t_F + 5\tau)$.

3.3. SHEATH STRUCTURE AND ELECTRON THERMALIZATION

One dimensional, collisionless models[3,12] of the longitudinal autoneutralization process have shown that the voltage in the sheath rises from zero at the ground plane ($x = 0$) and oscillates with a spatial period of $.2h_{DL}$ and peak to trough amplitude of $4V_s$ about a D.C. level of $V_s = \mu E_K$. The basic physics involved here is described by Chen as an ion acoustic shock wave.[13] These voltage oscillations decay within 2.5 periods even in a collisionless sheath. This decay does not show up in collisionless analytical models.[12] (See Fig. 2.) The dissipation mechanism involved appears to be a velocity space instability of the electron distribution function, essentially the two stream instability.[3,14] Fast

electrons near the voltage peaks ($V \simeq 4V_s$, $v_e \simeq 2v_+$) race into slow electrons in the troughs ($V \simeq 0$, $v_e \simeq 0$). Electrons thermalize producing a velocity spread about mean directed energy V_s at velocity v_+. One dimensional, time dependent computer simulations of the electron velocity distributions have shown this velocity spread to be $.61v_+$ full width at half maximum.[3] Dividing this thermal energy into three spatial modes means that the electron temperature in a plasma flow ($x > .5h_{DL}$) resulting from autoneutralization is[3]

$$T_e = .043\ V_s = .043\ \mu\ E_K \quad \text{volts} \quad . \tag{3.3.1}$$

Example 3.

In a plasma flow produced by the autoneutralization of the 20 MeV, 50 A/cm^2 ion beam of example 1 the electron temperature and electron thermal (i.e. transverse) speed are:

$$T_e = 468 \text{ volts}$$

$$v_{e_{th}} = 4.17 \times 10^7 \sqrt{\frac{8T_e}{\pi} \text{ in volts}} \quad \frac{\text{cm}}{\text{sec}} = 4.17 \times 10^7 \sqrt{.043\ \frac{8V_s}{\pi}} \quad \frac{\text{cm}}{\text{sec}}$$

$$= 1.44 \times 10^9 \text{ cm/sec} \quad . \tag{3.3.2}$$

3.4. SUMMARY

Over distances greater than $\sim .5h_{DL}$ and times less than $(t_F + \tau)$ a charge ($n_e = n_+$) and current ($v_e = v_+$) neutralized one

dimensional plasma flow at space potential $V_s = (m_e/m_+)E_K$ and electron temperature $T_e = .043V_s$ is available for measurement. A floating potential probe, sampling the outer edges of this beam can produce a signal directly proportional to ion energy, with ns resolution and survive during the residence time of the beam pulse without altering the plasma properties. The floating potential probe is described in the following section.

For times greater than $(t_F + 5\tau)$ a stream of positive current $I_+ = j_+\pi D^2/4$ propagates through a stationary electron cloud with zero net space charge ($n_e = n_+$) and at $V_s = .38\ \mu E_K$.* Closed "drift tube" Faraday cup probes can measure a time averaged ion energy and time resolved ion current.

* This is a guess:

1) if all (1D) k.e. goes into random (3D) motion:

$$T_e^*(t \sim t_F+\tau) = \frac{1}{3} V_s(t=0) = \frac{\mu E_K}{3}$$

2) as T_e grows V_s decays; less I_e need be extracted from the drift tube walls to neutralize the positive beam, a guess at time averaged T_e resulting after $t_F + 5\tau$ is $\frac{1}{2} T_e^*(t_F+\tau)$:
$T_{e_{FINAL}} = \frac{1}{6} V_{s_{INITIAL}} = \frac{\mu E_K}{6}$

3) final space potential $V_s(t>t_F+5\tau) \simeq 2.3\ T_{e_{FINAL}} \simeq \frac{2.3}{6} \mu E_K$
$V_{s_{FINAL}} = .38\ \mu E_K$.

4. THE FLOATING PROBE

4.1. RANDOM FLUXES

Consider an inertial reference frame F_1 fixed to the mass motion of a plasma flow with velocity v_+. In this frame of reference only thermal motion of particles is observed. The random particle flux of species s crossing a unit area in one direction is[15]

$$\Gamma_s = \frac{n_s \, v_{s_{th}}}{4} \quad . \tag{4.1.1}$$

The factor of 1/4 is comprised of two factors of 1/2. The first accounts for the fact that at the surface only 1/2 of species s particles have velocity components into the surface. The second factor of 1/2 is the average of the direction cosine over a hemisphere. As long as

$$\frac{T_e}{T_+} > \frac{m_e}{m_+} \tag{4.1.2}$$

electron thermal velocity $v_{e_{th}}$ will be larger than ion thermal velocity $v_{+_{th}}$ and $\Gamma_e > \Gamma_+$. The ion temperature in condition (4.1.2) should characterize actual ion thermal motion instead of being a geometric divergence parameter based on cold ion ballistic trajectories.

Example 4.

$T_e = 468$ V

$T_+ = 18.5$ keV (thermal divergence)

$n_e = n_+ = 5.12 \times 10^{10}$ cm^{-3}

$h_{De} = .071$ cm

$v_{e_{th}} = 1.44 \times 10^9$ cm/sec.

$v_{+_{th}} = 2.13 \times 10^8$ cm/sec.

$v_{e_{th}} > v_{+_{th}}$ if $T_+ < 849$ keV

$$\left|j_{e_{th}}\right| = e\Gamma_e = 2.953 \text{ A/cm}^2$$

$$\left|j_{+_{th}}\right| = e\Gamma_+ = .437 \text{ A/cm}^2 .$$

Generally $v_{e_{th}} >> v_{+_{th}}$ and electron space charge rapidly adjusts to the comparatively slow motion of the ions.

4.2. FLOATING POTENTIAL

Now consider an isolated absorbing body suspended in F_1. (See (16) for similar discussion.) The total electron and ion currents crossing the body surface are the random fluxes times the body surface area A_p:

$$I_{e_{th}} = -e\Gamma_e A_p \qquad (4.2.1)$$

$$I_{+_{th}} = e\Gamma_+ A_p \quad . \qquad (4.2.2)$$

Since electrons travel faster than ions the body soon accumulates a negative charge with respect to the plasma. As the plasma has a uniform space potential of V_s the body must develop a potential $V_F < V_s$. The potential drop $V_s - V_F$ is confined to a sheath several Debye lengths

$$h_{De} = \sqrt{\frac{\epsilon_0 T_e(\text{volts})}{e n_e}} \quad . \qquad (4.2.3)$$

thick. This sheath is an electron barrier which adjusts its thickness as well as the drop $V_s - V_F$ to exactly balance the electron and ion currents reaching the body. V_F, called the floating potential, is that voltage which a body in contact with a plasma assumes if it draws no net current. Clearly the magnitude of $V_s - V_F$ must be proportional to T_e.

4.3. ELECTRIC PROBE THEORY

The exact relationship between $V_s - V_F$ and T_e depends on the details of the sheath physics. This problem is quite involved and has spawned a complete literature.[15,17,18] However simple, approximate relationships $V_s - V_F(T_e)$ have been developed on the basis of Maxwell-Boltzmann statistics.[19] Precise estimates of $V_s - V_F(T_e)$ can be obtained by referring to the numerical results of rigorous probe theories.[20] Nevertheless, the approximation I will use should be more than

adequate for this discussion and in all probability for the interpretation of actual floating probe measurements (see Appendix 2).

$$V_s - V_F = -\frac{T_e}{2} \ln \left(\frac{T_+}{T_e} \frac{m_e}{m_+}\right) \quad . \tag{4.3.1}$$

4.4. AN ION ENERGY PROBE

A floating probe can look like a conventional spark plug without the ground electrode. A center conductor surrounded by an insulating sleeve pokes through the drift tube wall and the exposed center conductor extends into the plasma. The center conductor is connected to ground through a resistor R_p sized such that the probe current I_p is small with respect to electron thermal (electron saturation) current:

$$I_p = V_F/R_p \ll |I_{e_{th}} = -eF_e A_p| \quad . \tag{4.4.1}$$

The floating probe measures voltage and voltage probes draw as little current as possible. The chain of logic which gives time resolved E_K from $I_p(t)$ follows:

$$V_F = I_p R_p \tag{4.4.2}$$

$$V_F = V_s + \frac{T_e}{2} \ln \left(\frac{T_+}{T_e} \frac{m_e}{m_+}\right) \tag{4.4.3}$$

$$V_F = V_s \left(1 + .0215 \ln \left(\frac{\pi d\theta^2}{.172}\right)\right) \tag{A2.4b}$$

$$E_K = \frac{V_F}{\mu\left(1 + .0215 \ln\left(\frac{\pi d\theta^2}{.172}\right)\right)} \quad . \tag{4.4.4}$$

Essentially, the floating probe is the second stage of a $\mu \equiv \frac{m_e}{m_+}$ voltage divider; E_K is divided by autoneutralization to $V_s = \mu E_K$ and the floating probe measures V_F, related to V_s by a constant.

Example 5.

E_K = 20 MeV protons

T_+ = 18.5 keV; $d\theta = 2^0$

V_S = 10.89 kV

V_F = 10.00 kV (92% of V_s)

$j_{e_{th}} = 2.953\ A/cm^2$

h_{De} = .071 cm (negligible effect on Ap in this example)

for a probe:

$A_p = 3.39\ cm^2$ (2.0" diam disc, or 1" x .5" plate)

$R_{p_{min}}$ = 10 kΩ have: $I_{e_{th}}$ = 10A, $I_{p_{max}}$ = 1 A < $I_{e_{th}}$,

$P_{p_{max}}$ = 10 kW .

A 1 A signal with a 10 kW heat dissipation is a reasonable engineering criteria.

Spatial resolution is improved and beam interference is minimized by reducing probe area and consequently signal. This spatial resolution-signal amplitude trade-off as well as the ability of the probe collecting area to

survive in the beam and the probe circuit to respond quickly relative to the beam pulse length are the major limitations of the floating probe.

4.5. TIME RESPONSE

After the initial transients due to the beam front impacting the probe the sheath changes slowly with ion temperature fluctuations.[21] The floating potential can adjust to changes in the space potential on a time scale determined by electron inertia. This lag time t_p is proportional to the electron transit time across the sheath and has been estimated on the basis of experience[21]

$$\frac{2\pi}{\omega_{pe}} = \frac{1}{8980\sqrt{n_e cm^{-3}}} \leq t_p \leq \sim 10 \text{ ns} \qquad (4.5.1)$$

where ω_{pe} is the electron plasma frequency $\left(\frac{2\pi}{\omega_{pe}} \sim .5 \text{ ns for } n_e = 5.12 \times 10^{10} \text{ cm}^{-3}\right)$.

The stray capacitance C_p of the wire to a probe limits the response time to $\tau_{RC} = R_p C_p$. For a response of 1 ns with R_p = 10 kΩ, C_p must be at most .1 μF. A 60 kΩ probe, consisting of a .5 mm diam tungsten wire in a pyrex sleeve, with a response time of approximately 10 ns (estimated C_p = .17 μF) has been reported.[26]

An experimental difficulty with floating probes can be radio noise pickup. Noise becomes a problem when its frequency matches the ion or electron plasma frequencies:

$$\nu_{p_{+0}} = 209.5\sqrt{n_+ \text{ cm}^{-3}} \quad \text{Hz} \quad (= 47 \text{ MHz})\ ^{(9)} \tag{4.5.2}$$

$$\nu_{p_{e0}} = 8980\sqrt{n_e \text{ cm}^{-3}} \quad \text{Hz} \quad (= 2032 \text{ MHz}).^{(9)} \tag{4.5.3}$$

Experiments have shown that electric probes perform quite well in the presence of non-resonant noise and are routinely used to detect waves and discrete oscillations.[21]

4.6. SUMMARY

A floating potential probe, sampling the outer edges of the beam can produce a signal directly proportional to ion energy, with ns resolution. This constant of proportionality embodies the electron temperature which results from autoneutralization and its relationship to the sheath potential drop. Both of these quantities are calculated from theory and to that extent are uncertain (experiments are generally supportive). However because the electron temperature T_e is so low compared to the space potential V_s, the floating potential V_F will always be between .92 and .84 of V_s and the proton kinetic energy E_K can be determined to within 10% from (see Appendix 2)

$$E_K = \left(\frac{m_+}{m_e}\right) V_F \ (1.09\ ^{+.1}_{-0.}) \quad . \tag{4.6.1}$$

5. BEAM-MATERIAL INTERACTION

5.1. INTERACTION CONDITION

One of the concerns of any ion beam experiment is whether probes and collimators can withstand the energy loading during the lifetime of the beam τ_B without degradation in performance or alteration of beam properties.

Let ε_c be the critical energy per atom that a material can absorb before the onset of undesirable beam-surface interactions. ε_c is a parameter of convenience which can characterize melting, ablation or other process of concern. Ions transmit the energy flux of the beam, which is:

$$P = j_+ E_K \quad \text{watts/cm}^2 \quad . \tag{5.1.1}$$

During the extent of a beam pulse τ_B (sec.) the energy per unit area delivered through a surface is $P\tau_B$. The range, or depth of penetration of ions into a material, is a function of ion energy and will be denoted by l_+. The beam-material interaction condition can be stated as follows:

$$\begin{matrix}\text{no interaction} \\ \text{if } l\end{matrix} \quad < \frac{\varepsilon_c}{\varepsilon_B} = \frac{\varepsilon_c}{\left(\frac{P\tau_B}{l_+ N}\right)} < \begin{matrix}\text{surface interaction} \\ \text{if } l\end{matrix} \tag{5.1.2}$$

where

$N = \frac{\rho N_0}{A_w}$ (cm^{-3}) is the atom density of the material.

$N_0 = 6.022 \times 10^{23}$ $(\text{gm-mole})^{-1}$ is Avogadro's No.

A_w = atomic weight (gm/mole) of the material.

ρ = mass density (gm/cm^3) of the material.

This condition states that when the average energy gain per atom of material (ϵ_B) in a surface layer one ion penetration depth (l_+) thick is less than ϵ_c that no beam-surface interaction will occur before time τ_B. The time required for each particle in an ion penetration surface layer to absorb an average energy ϵ_c is

$$\tau_c = \frac{\epsilon_c}{\left(\frac{P}{Nl_+}\right)} \quad . \tag{5.1.3}$$

Beam-surface interactions are forstalled by using light (low A_w, thus high N), refractory (high ϵ_c) materials and low power, high energy (large l_+) beams. This distributes beam energy to a deeper and numerically denser layer. It is interesting to note that experiments with intense, low energy ion beams and heavy metal collimators create an overwhelming beam-surface interaction.[5]

For:

P watts/cm^2

N cm^{-3}

l_+ cm .

$$\tau_c = \left(\frac{Nl_+}{P}\right) \quad \left(\epsilon_c = eV_c = kT_c^{\circ}\right) \tag{5.1.4}$$

where

ϵ_c joules

V_c volts

T_c° °K

$e = 1.6021 \times 10^{-19}$ Joule/eV

$k = 1.3807 \times 10^{-23}$ °K/Joule (Boltzmann's constant).

5.2. *ION RANGE AND INVERSE ATOMIC AREA (Nl_+)*

Example 6.

The interaction condition will be illustrated by two examples:

6a) 20 MeV protons at 50 A/cm^2, P = 1 GW/cm^2.

6b) .5 keV alphas at 248 kA/cm^2, P = .124 GW/cm^2.

6a) Protons:

Material density ρ (gm/cm^3), atomic weight A_w (gm/mole) and proton range l_+ (20 MeV) (cm) data from Janni[22] have been used to calculate atom density N (atoms/cm^3), the range parameter $l_+\rho/\sqrt{A_w}$ and "inverse atomic area" Nl_+ (cm^{-2}) for ten materials. (See Table 1.) A common assumption in ion range estimation is that $l_+\rho/\sqrt{A_w}$ is constant for all materials for a specific ionic species and energy.[23] It can be seen from Table 1 that $l_+\rho/\sqrt{A_w}$ varies by a factor of two over four decades of material density.

6b) Alphas:

Alpha particles will be used to model a helium ion beam in which pronounced beam-surface interactions were observed.[5] Given the constancy of $l_+\rho/\sqrt{A_w}$ and the datum:[24] 1 keV alpha particles have a 2 to 3 cm

TABLE 1. 20 MeV protons.

Material	ρ gm/cm^3	A_w gm/mole	$N/10^{22}$ atom/cm^3	l_+ cm	$\frac{l_+\rho}{\sqrt{A_w}}$ $\frac{\sqrt{\text{gm-mole}}}{\text{cm}^2}$	$l_+N/10^{22}$ atoms/cm^2
N_2	1.2504×10^{-3}	14.007	5.3×10^{-3}	388	.130	2.09
Air	1.29×10^{-3}	15.13	5.13×10^{-3}	379	.126	1.94
C	2.22	12.011	11.1	.21301	.136	2.36
B	2.3	10.811	12.8	.2176	.152	2.79
Al	2.699	26.981	6.02	.21113	.110	1.27
Fe	7.87	55.847	8.49	.08486	.0894	.72
Cu	8.92	63.54	8.45	.07947	.0889	.672
Pb	11.34	207.19	3.30	.09529	.0751	.314
U	18.7	238.03	4.73	.06173	.0748	.292
W	19.3	183.85	6.32	.05324	.0758	.336

range in air at standard temperature and pressure; one estimate of sub-kilovolt alpha particle range is:

$$l_\alpha = (6.63 \times 10^{-4}) \frac{\sqrt{A_w}}{\rho \ (\text{gm/cm}^2)} \text{ cm} \quad . \tag{5.2.1}$$

Table 2 lists estimates of l_α and Nl_α for sub-kilovolt alphas in aluminium, copper, and tungsten.

TABLE 2. Sub-kilovolt alphas.

Material	l_α(cm)	$Nl_\alpha/10^{19}$ (cm^{-2})
Al	1.28×10^{-3}	7.69
Cu	5.93×10^{-4}	5.01
W	4.66×10^{-4}	2.95

5.3. MATERIAL HEATING

From Eq. (5.1.4) one can calculate the time (ns) required for a given temperature increase per particle in a surface layer of depth l_+ and its inverse, the temperature rise per particle per ns for the layer. These results are shown in Table 3, the top ten entries for example a) protons and the last three for example b) alphas.

Because of their limited penetration low energy ion beams create shallow layers of high energy density material. With the greater depth of their penetration high energy ion beams of comparable power dissipate through more material and are less likely to cause melting and ablation. From Table 3 it is also clear that boron and carbon are much more resistant to energy loading than the heavy metals. Boron nitride has been successfully tested in Tokamak environments[25] and is commonly used in the plasma propulsion thruster at Princeton University. With a maximum operating temperature of 2000 °C, boron nitride would make an excellent collimator and probe sleeve material for high energy ion beam experiments. After a 100 ns pulse of 50 A/cm^2, 20 MeV protons a boron nitride target would only heat up about 300 °K.

TABLE 3. Material surface heating.

Material	ns/°K	°K/ns	°K @ 100 ns = τ_B
N_2	.29	3.47	
Air	.27	3.73	For τ_B = 100 ns
C	.33	3.07	
B	.39	2.60	Boron and carbon heat
Al	.18	5.70	up by about 300 °K
Fe	.10	10.06	Al, Cu, and Fe from 500 to
Cu	.09	10.78	1000 °K temperature rise
Pb	.04	23.07	and the heavy metals
U	.04	24.80	reach melting conditions.
W	.05	21.56	
			°K @ 1 μs = τ_B(5)
Al	8.6×10^{-3}	117	10 to 30 ev/particle!
Cu	5.7×10^{-3}	179	Clearly melting, ablation
W	3.3×10^{-3}	304	and surface plasma occur.

5.4 SUMMARY

... total pulse energy loading $P\tau_B$ (joule/cm^2) less than $\epsilon_c N1_+$ no ...-surface interaction will affect beam or target properties. ... energy loading greater than this, melting, ablation and surface plasma ...fects must be expected.

6. TRANSVERSE MAGNETIC FIELDS

One way to measure directed ion energy is to deflect the plasma stream with a transverse magnetic field onto an array of detectors. To be successful such a scheme must suppress beam polarization drift with large, heavy magnets.

6.1. POLARIZATION DRIFT

A plasma beam may propagate without deflection through a region of transverse magnetic field B when its dielectric constant ϵ/ϵ_0 is significantly larger than $\sqrt{m_+/m_e} = \sqrt{1/\mu}$ (26):

$$\frac{\epsilon}{\epsilon_0} = 1 + \left(\frac{\omega_{p+}}{\omega_{c+}}\right)^2 = 1 + \left(\frac{\nu_{p+0}}{\nu_{c+0}}\right)^2 \left(1 + \frac{E_K}{E_0}\right) \gg \sqrt{\frac{m_+}{m_e}} \qquad (6.1.1)$$

where

$$\nu_{p+} = \frac{1}{2\pi}\sqrt{\frac{e^2 n_+}{\epsilon_0 m_+}} = \left(\frac{\omega_{p+0}}{2\pi}\right)\frac{1}{\sqrt{\frac{E_K}{E_0}+1}} = \frac{209.5\sqrt{n_+\ \mathrm{cm}^{-3}}}{\sqrt{\frac{E_K}{E_0}+1}}\ \mathrm{Hz} \qquad (6.1.2)$$

is the ion plasma frequency (last entry for protons) and

$$\nu_{c+} = \frac{1}{2\pi}\frac{eB}{m_+} = \left(\frac{\omega_{p+0}}{2\pi}\right)\frac{1}{\left(\frac{E_K}{E_0}+1\right)} = \frac{1525\ B(\mathrm{Gauss})}{\left(\frac{E_K}{E_0}+1\right)}\ \mathrm{Hz} \qquad (6.1.3)$$

is the ion cyclotron frequency (last entry for protons)

and

E_K = ion kinetic energy

E_0 = ion rest mass energy

(938.256 MeV for protons)

subscript "0" means "at rest."

When condition (6.1.1) obtains, an electric field perpendicular to both v and B is formed of magnitude E = vB and the beam propagates across the magnetic field by a polarization drift. Condition (6.1.1) can be recast as

$$B \ll B_L = \sqrt{\frac{n_+ m_{+0}}{\epsilon_0}} \sqrt{\frac{1 + E_K/E_0}{\sqrt{m_{+0}/m_e}\sqrt{1 + E_K/E_0} - 1}} \quad . \tag{6.1.4}$$

The polarization drift occurs when an imposed, transverse magnetic field B is less than B_L (L for Lorentz).

For protons:

$$B_L \text{ (Gauss)} = .13738 \sqrt{n_+ \text{ cm}^{-3}} \sqrt{\frac{1 + \frac{E_K}{938.256 \text{ MeV}}}{42.85\sqrt{1 + \frac{E_K}{938.256 \text{ MeV}}} - 1}} \tag{6.1.5}$$

Example 7

What is B_L in a 20 MeV proton beam with 5.12×10^{10} $cm^{-3} = n_+ = n_e$?

$B_L = 4.830$ kG.

To deflect this beam and suppress the polarization drift, B should be 4.83 kG or larger.

TABLE 4. B_L for various E_K at $n_+ = 5.12 \times 10^{10}$ cm^{-3}.

B in kG	E_K in MeV
4.806	1
4.818	10
4.830	20
4.866	50
4.925	100

6.2. DEFLECTION TRIGONOMETRY

A plasma beam with ions of rest energy E_0 and kinetic energy E_K is to be deflected a lateral distance y_s by a transverse magnetic field B larger than B_L. The axial distance required for this deflection is

$$x_s = \sqrt{y_s(2r_{c+}-y_s)} = \sqrt{y_s\left[\frac{2c}{\left(\frac{eB}{m_{+0}}\right)}\sqrt{\left(\frac{E_K}{E_0}+1\right)^2 - 1} - y_s\right]} \qquad (6.2.1)$$

where

r_{c+} is the ion gyroradius

c is the speed of light.

For protons

$$x_s = \sqrt{y_s\left(\frac{6.260 \times 10^6}{B\ (\text{Gauss})}\sqrt{\left(\frac{E_K\ (\text{MeV})}{938.256}+1\right)^2 - 1} - y_s\right)} \quad \text{cm} \quad . \quad (6.2.2)$$

TABLE 5. x_s (cm) at three y_s for B = 6 KG $\geq B_L(n_+, E_K)$.

Lateral deflection: y_s	E_K in MeV, ion kinetic energy				
cm	1	10	20	50	100
1	6.9	12.3	14.7	18.6	22.2
5	14.7	27.2	32.5	41.2	49.5
10	19.5	37.8	45.4	57.9	69.6

6.3. A POLARIZATION FIELD DOUBLE PROBE

A double floating probe can be used to measure the polarization electric field that results in an undeflected plasma stream in a region of transverse magnetic field $B < B_L$.[26,29] This measurement can be used to determine the stream velocity and hence ion energy.

$$E = \left| \frac{V_{F_1} - V_{F_2}}{\text{Probe Separation}} \right| = v_+ B \tag{6.3.1}$$

$$v_+ = \frac{E}{B} \quad . \tag{6.3.2}$$

Any systematic noise picked up by the floating probes in the magnetized plasma should be cancelled out by the differencing. It is expected that magnetized plasma streams will be generally noisier than unmagnetized ones, thus the successful measurement of time dependent floating potentials and polarization fields[26,29] is encouraging from the point of view of Section 4.

6.4. SUMMARY

The problems in building an ion deflecting magnetic spectrometer are:

1. large magnetic fields ($\sim$6 KG for $E_K \sim$ MeV's $n_+ \sim 10^{10}$ cm^{-3}) are necessary to suppress polarization drift.
2. large area ($>\sim$100 cm^2) and consequently heavy magnets are required for reasonable energy discrimination ($\sim$1 MeV/cm).

A double floating probe can measure the polarization field in the beam which is a direct measure of the ion velocity and hence ion directed energy.

7. THE DIAGNOSTIC POSSIBILITIES

7.1. General Survey

The following survey of diagnostic methods and their limitations is based on a similar discussion by Humphries.[27]

a. Calorimetry

Not recommended for ion beams. Ablation of target material carries off energy and confuses diagnosis.

b. Net Current Probe

Positive charge is collected in a Faraday cup. The charge collector must have a negative bias V_c such that $V_c < 0$ to repel j_e (Section 3.1); or the Faraday cup must be in a shielded enclosure in which current neutralization quickly decays (Section 3.2); or the Faraday cup must be electron magnetically insulated (Appendix 3.). The filter or shield in front of the Faraday cup will stop ions whose range l_+ is less than the filter thickness l_c. Several such detectors can be combined to deduce a temporal energy spectrum by differencing signals to construct energy bins. Also, monitoring current neutralization decay in one detector gives an estimate of time averaged ion energy.

c. Witness Plates

Metal tabs strategically located record the extent of ion bombardment. This measurement is qualitative, ambiguous, time integrated and not prompt.

d. Nuclear Activition

This method has wide utility, is time integrated and not prompt.

e. Neutron Production

A deuterated film on the accelerator anode creates a deuteron beam which collides into a deuterated target producing a neutron beam which is measured and analyzed. This method is indirect, complex and depends on many calibrations.

f. Prompt γ-rays

Ion bombardment of an appropriate target induces nuclear transmutation reactions which liberate γ-rays. Large ion current densities are required for measurable γ signals; it is difficult to calibrate absolutely for flux measurements and radiation detectors must be shielded from accelerator x rays.

g. Atomic Line Excitation

Collisionally induced atomic line radiation is sensitive to ion energy and obscured by plasma absorption. Complex analysis is required.

h. Scintillator

For low current densities scintillator response is proportional to deposited beam energy. Beam attenuation has an uncertain effect on beam propagation hence low current density diagnostics on highly attenuated beams are only qualitative. Scintillators can be used to measure the time of flight of the head of the beam.

i. Target Response

Ion energy can be infered by monitoring the motion, shocks in and thermal radiation from a target. Complex hydrodynamic codes are required.

j. Rutherford Scattering Spectrometer[28]

A target foil is placed in the beam at a 45° angle. Ions, Rutherford scattered at 90° from the beam, are magnetically analyzed by an array of PIN diodes. Only a small fraction of beam ions are sampled. The threshold of detector sensitivity places a requirement of minimum beam current density. Time dependent ion beam energy translates into a sweeping of the Rutherford scattered beamlet across the PIN diode array. Plans call for a 6 KG .5" diameter permanent magnet to deflect ions and trap what few stay electrons appear.

k. $\dot{B}$ Loops

It might be possible to monitor neutralization currents in drift tube walls with $\dot{B}$ loops.

l. Ion Spectrometer

The deflection of MeV beam ions directly onto a detector array requires large heavy magnets capable of overcoming the polarization drift.

m. Floating Probes

These are discussed in Section 4. Double floating probes have been used successfully to temporally monitor the polarization electric field in magnetized plasma beams.[26,29] The floating potentials observed tracked the ion source accelerating potential but floating potential magnitude was too high due to the imposed magnetic field.[30] I am attempting to persuade the authors of these studies

to run experiments without magnetic fields that test

$$E_K = V_F \left(\frac{m_+}{m_e}\right) \left(1.09 \begin{smallmatrix} +.1 \\ -0. \end{smallmatrix}\right) \text{ for protons.}$$

The diagnostics which appear to be most promising as straightforward, prompt, time dependent energy measurements are:

i) net current probes;

ii) Rutherford Scattering Spectrometer; and

iii) floating probes.

7.2. Summary

Net current probes, the Rutherford Scattering spectrometer and floating probes are the most promising diagnostics for prompt, time dependent measurement of ion directed energy.

A radial array of negatively biased, ion range filtered, net current probes can measure a time dependent energy spectrum. An axial array can measure beam time of flight. An unbiased, shielded net current probe can be constructed to monitor the decay of current neutralization and then ion flux. Time averaged ion energy and time dependent current density are measured in this way. The drift tube enclosing the ion beam could be used as a current neutralization decay monitor.

The Rutherford Scattering spectrometer being developed by Ramon Leeper at Sandia National Laboratory, Albuquerque should measure time dependent directed ion energy in beams of sufficient current density.

A single floating probe in a non-magnetized, current neutralized plasma stream should give a time dependent measurement of directed ion energy within 10% without requiring calibration or analysis.

8. SYNOPSIS OF CONCLUSIONS

1. High current density ion beams will be charge and current neutralized.
2. Current neutralization will decay on a time scale determined by drift tube geometry.
3. The electron temperature resulting from autoneutralization remains unchanged (collisionless) and significantly less than other temperatures and kinetic energies (T_+, E_K, V_S).
4. Floating potential is nearly identical with space potential and a floating probe in a current neutralized beam will give ion directed energy to within 10%; for protons:

$$E_K \approx V_F \left(\frac{m_+}{m_e}\right) \left(1.09 \begin{matrix} + .1 \\ - 0. \end{matrix}\right) \quad .$$

5. The decay of current neutralization can be used as a time integrated ion directed energy diagnostic.
6. Collimation of pulsed multi-keV beams can create plasmadynamic expansions and serious alterations of beam properties. Pulsed, multi-MeV beams should be safe from this concern.
7. Magnetic deflection of high current density MeV ion beams for spectroscopic analysis is impractical, but is ideal for low current density situations. Beam attenuation may permit magnetic spectroscopy
8. Promising diagnostics for time dependent ion directed energy measurement are: i) shielded/range filter ion and net current probes
   ii) Rutherford Scattering spectrometer
   iii) single floating probe.

REFERENCES

1. Stanley Humphries, Jr. "Intense Pulsed Ion Beams for Fusion Applications" Nuclear Fusion, Vol. 20, No. 12 (1980) p. 1549.
2. J. Maenchen, L. G. Wiley, S. Humphries, Jr., E. Peleg, R. N. Sudan, P. A. Hammer "Magnetic Focusing of Intense Ion Beams" Phys. Fluids 22 (3) March 1979 p. 555 (see Section III).
3. S. Humphries, Jr., T. R. Lockner, J. W. Poukey, J. P. Quintenz "One-Dimensional Ion-Beam Neutralization by Cold Elections" Phys. Rev. Lett. 46 (15) 13 April 81 p. 995.
4. Stanley Humphries, Jr., Thomas R. Lockner "High Power Pulsed Ion Beam Acceleration and Transport" Sandia Report SAND81-2009 Nov. 1981
5. Rachid Mesli, Altan M. Ferendeci, O. K. Mawardi "Plasma-Beam-Hole Interaction" IEEE Transactions on Plasma Science Vol. PS-9, No. 2 June 1981 p. 58.
6. See Ref. 4 pp. 15 - 17; see Ref. 2 p. 559 Eq (3); see Ref. 1 pp. 1577 - 1578 Sec. 5.1.
7. See Ref. 1 especially Section 5.1 pp. 1577 - 1580, see Ref. 2 especially Section III; see Ref. 4 pp. 16 - 41.
8. I will use the word plasma rather than lengthy euphemisms such as "neutralized ion beam" or "ion beam with an equivalent number of co-moving electrons". In any event I will be concerned with beams which are longer than h_{DL} and wider than h_{DT}. It will be useful to view these beams as supersonic plasma flows.
9. Refers to 20 MeV, 50 A/cm^2 reference ion beam of example 1.

10. See Ref. 1 p. 1578; see Ref. 4 pp. 39-41.

11. A. T. Drobot, S. A. Goldstein, R. Lee "Simulation of a Current Probe for Intense Ion Beams" Am. Phys. Soc. Bull. 23 (1978) pg 816. This reference is duplicated in full: 5D12 Simulation of a Current Probe for Intense Ion Beams*. A. T. DROBOT, SHYKE A. GOLDSTEIN, Science Applications, Inc., and ROSWELL LEE, Naval Research Lab.--Recent advances in the understanding of high voltage diode physics has made possible the efficient production of tense ion beams. It has however been difficult to measure the time resolved ion current and energy spectrum. The primary difficulty with biased Faraday cups or magnetic loops is that neutralizing and secondary electrons distort the true current measurement. We have successfully simulated a simple probe that promises to yield the correct time resolved ion current and can also be used to determine the energy spectrum. The probe is a small cavity collector into which the ion beams passes through a thin KimFol foil. Using one-dimensional particle motion and two-dimensional electromagnetic field solutions we have found that the current collected, after a short transient, is just the bare ion current. Further work with two-dimensional particle orbits is in progress and will be reported on. *Work supported by the Defense Nuclear Agency and the U. S. Department of Energy, Wash., D.C.

12. E. Stuhlinger, Ion Propulsion for Space Flight (McGraw-Hill, NY 1964). This reference was cited in Ref. 3 (also 1 and 4). Stuhlinger shows a voltage - distance solution which oscillates between 0 and $4V_s$ and extends to infinity. He derives this from a one-dimensional steady-state collisionless analytical model. Humphries et al., Ref. 3, show damped

oscillations; the first voltage peak of $V \simeq 4V_s$ at $x \simeq .1h_{DL}$, the second of amplitudes $2V_s$ at $x \simeq .3h_{DL}$ and a decay of voltage peaks to the D.C. level of V_s from $x \simeq .3h_{DL}$ to $x \simeq .5h_{DL}$. The computer simulation used was one-dimensional, time dependent and contained dissipation.

13. F. F. Chen, Introduction to Plasma Physics (Plenum Press, NY 1976) pp. 249-252.
14. B. Sam. Tanenbaum, Plasma Physics (McGraw-Hill, NY 1967) pp. 198-202; see Ref. 13 pp. 186-190.
15. Frances F. Chen, "Electric Probes", Chapter 4 in Plasma Diagnostic Techniques, eds: R. H. Huddlestone, S. L. Leonard, Academic Press, New York 1965 p. 126.
16. See Ref. 13 p. 244.
17. J. D. Swift, M. J. R. Schwar, Electric Probes for Plasma Diagnostics American Elsevier, New York 1969.
18. Paul M. Chung, Lawrence Talbot, Kenell J. Touryan, Electric Probes in Stationary and Flowing Plasma: Theory and Applications, Springer-Verlag, New York 1975.
19. See Ref. 15 pp. 177-178; see Ref. 14 pp. 213-215; see Ref. 17 p. 15.
20. See Ref. 18 p. 20, especially footnote.
21. See Ref. 15 p. 188; see Section 7 pp. 185-191.
22. Joseph F. Janni "Calculations of Energy Loss, Range, Pathlength, Straggling, Multiple Scattering and Probability of Inelastic Nuclear Collisions for 0.1 to 1000 MeV Protons" AFWL-TR-65-150 Sept. 1966.
23. William J. Price, Nuclear Radiation Detection, (McGraw-Hill, NY) 1964 p. 9.

24. Thank you Hazards Control - Health Physics (29 July 1982 telephone communication).

25. P. D. Coleman, B. D. Blackwell, M. Kristiansen, M. O. Hagler, "Investigations of Various Probe Sheath Materials in the Texas Tech Tokamak" IEEE Transactions on Plasma Science Vol. PS-9, No. 3 Sept. 1981 p. 123.

26. T. Ikehata, K. Kamada, H. Ishizuka, T. Kawabe, S. Miyoshi, "Observation of the polarization electric field in the intense neutralized proton beam propagating undeflectedly across a magnetic field". Phys. Rev. A. Vol. 25, No. 6 p. 3415 June 1982.

27. See Ref. 1 pp. 1573-1577 Section 4.

28. This diagnostic is being developed by Ramon Leeper at Sandia National Laboratories in Albuquerque, New Mexico.

29. S. Robertson, H. Ishizuka, W. Peter, N. Rostoker, "Propagation of an Intense Ion Beam Transverse to a Magnetic Field" Phys. Rev. Lett. Vol 47 No. 7 p. 508 17 Aug. 1981.

30. A telephone conversation with T. Kawabe and T. Ikehata (11 Aug 1982) reveals that the zero B field floating potentials observed are significantly higher (~1kV) than my estimate of $V_s = \mu E_K$ (≈40 to 150 V). Yet the negative bias imposed on their ion current collecting probe is only -300 V which by my guess should be $\leq -V_s$ to effectively repel all electrons with a potential barrier equal to $2V_s$. However, I am too far removed from this experiment, both by distance and direct experience to adequately compare it with the analysis I present. I am sure the reactions of T. Kawabe, and T. Ikehata, as well as S. Robertson and T. Ishizuka to this report will be very instructive.

APPENDIX 1. DIVERGENCE ANGLE AND THERMAL VELOCITY

The divergence of a beam will be treated as if it were due entirely to ion thermal motion. Any given beam will diverge due to a combination of ion thermal motion and ion ballistics through the accelerator. For small half angles $d\theta$:

$$\frac{v_{+_{th}}}{v_+} = d\theta = \sqrt{\frac{8/\pi}{c}} \sqrt{\frac{kT_+^0 / m_{+0}}{1 - \left(\frac{E_K}{E_0} + 1\right)^{-2}}} = \sqrt{\frac{8}{\pi}} \sqrt{\frac{T_+ / E_0}{1 - \left(\frac{E_K}{E_0} + 1\right)^{-2}}} \qquad \text{(A1.1)}$$

where

m_{+0} is used in $v_{+_{th}}$; $m_+ = 1.02\ m_{+0}$ at $v_+/c = .2$ for example 1.

$T_+ = \frac{kT_+^0}{e}$ is the ion temperature in eV, and $k = 1.3807 \times 10^{-23}$ J/°K (or 10^{-16} erg/°K);

$E_0 = m_{+0}c^2$ is the ion rest mass energy in eV;

$E_K = (m_+ - m_{+0})c^2$ is the ion kinetic energy in eV .

For $E_K/E_0 << 1$:

$$\frac{T_+}{E_K} \simeq \frac{\pi}{4} (d\theta)^2 \quad . \qquad \text{(A1.2)}$$

Example A1

A 20 MeV proton beam with a divergence half angle of 2° has:

$$v_+ = 6.09 \times 10^{10} \text{ cm/sec}$$

$$d\theta = .0349 \text{ radians}$$

$$v_{+_{th}} = 2.13 \times 10^{-8} \text{ cm/sec}$$

and from

$$v_{+_{th}} = 9.79 \times 10^5 \sqrt{\frac{8T_+}{\pi}} \text{ in eV} \tag{A1.3}$$

$$T_+ = 18.5 \text{ keV} .$$

The divergence of a beam will cause the number and current density to decrease with distance. The diameter versus x of a diverging beam is given by

$$\frac{D(x)}{D} = 1 + \frac{2\, v_{+_{th}}}{v_+} \frac{x}{D} \tag{A1.4}$$

where D is the diameter at x = 0.

If the thermal velocity $v_{+_{th}}$ is constant, the density will drop with x:

$$I_+ = e\, n_+(x)\, v_+ \frac{\pi}{4} D^2 \left(1 + \frac{2\, v_{+_{th}}}{v_+} \frac{x}{D}\right)^2 = \text{constant} \tag{A1.5}$$

and

$$n_+(x) = \frac{I_+ \Big/ ev_+ \frac{\pi}{4} D^2}{\left(1 + \frac{2v_{+_{th}}}{v_+} \frac{x}{D}\right)^2} = \frac{n_{+0}}{\left(1 + \frac{2v_{+_{th}}}{v_+} \frac{x}{D}\right)^2} \qquad (A1.6)$$

Also

$$j_+(x) = \frac{en_{+0}v_+ \equiv j_{+0}}{\left(1 + \frac{2v_{+_{th}}}{v_+} \frac{x}{D}\right)^2} \qquad (A1.7)$$

This number and current density decrease should be kept in mind when working examples like those of the text. A beam which starts out as one dimensional ($h_{DT} < D_w$) and high current density ($h_{DL} < L$) may become three dimensional ($h_{DT} > D_w$) then low current density ($h_{DL} > L$) and thus non-neutral. The calculation of a neutralization decay (τ) time may be influenced by a beam divergence within a drift tube test cell. The performance of a floating probe, as well as the energy loading of material obstacles should be calculated on the basis of local beam properties.

APPENDIX 2. THE FLOATING POTENTIAL

Let $\xi = y/h_{De}$ be a coordinate normal to the probe surface which is zero at the probe and increasingly positive into the plasma. The electron barrier $V_s - V_F$ must be comparable to kT_e^0/e but as this is low compared to kT_+^0/e the sheath drop $V_s - V_F$ will not affect n_+, $v_{+_{th}}$ and thus $j_{+_{th}}$. The floating condition at $\xi = 0$ is:

$$j_{e_{th}} (\xi=0) = j_{+_{th}} \tag{A2.1a}$$

$$\frac{en_{e\infty}}{4} \exp\left[-\frac{e(V_s - V_F)}{kT_e^0}\right] \sqrt{\frac{8}{\pi}\frac{kT_e^0}{m_e}} = \frac{en_{+\infty}}{4}\sqrt{\frac{8}{\pi}\frac{kT_+^0}{m_+}} \tag{A2.1b}$$

Algebra follows:

$$\exp\left[-\frac{e(V_s - V_F)}{kT_e^0}\right] = \sqrt{\frac{T_+^0}{T_e^0}\frac{m_e}{m_+}} \tag{A2.2a}$$

as $n_{e\infty} = n_{+\infty}$. For T_e and T_+ in volts:

$$\exp\left[-\frac{V_s - V_F}{T_e}\right] = \sqrt{\frac{T_+}{T_e}\frac{m_e}{m_+}} \tag{A2.2b}$$

Finally:

$$V_F = V_s + \frac{T_e}{2} \ln\left(\frac{T_+}{T_e}\frac{m_e}{m_+}\right) \tag{A2.3}$$

This equation can be recast using (A1.2) and (3.31):

$$T_+ = \frac{\pi}{4} (d\theta)^2 E_K \qquad (A1.2)$$

$$T_e = .043 V_s = .043 \left(\frac{m_e}{m_+}\right) E_K \qquad (3.3.1)$$

to arrive at:

$$V_F = V_S \left[1 + .0215 \ln\left(\frac{T_+}{T_e} \frac{m_e}{m_+}\right)\right] \qquad (A2.4a)$$

$$V_F = V_s \left[1 + .0215 \ln \left(\frac{\pi (d\theta)^2}{.172}\right)\right] . \qquad (A2.4b)$$

The effect of T_+/T_e is small and is demonstrated by Table A1.

TABLE A.1. Effect of T_+/T_e on V_F/V_S for protons.

T_+/T_e	V_F/V_S	Equivalent $d\theta$
40	.92	1.98°
1	.84	.31°

In the neutralized ion beams under consideration

$$1 \ll \frac{T_+}{T_e} \ll \frac{m_+}{m_e} \quad , \tag{A2.5}$$

the electrons are cold compared to the ions but still exhibit higher thermal velocities. Also the electron directed energy V_s is significantly larger than the electron thermal energy T_e. Thus $V_s - V_F$ which is proportional to T_e should be negligible, which Table A.1 demonstrates. To determine E_K for protons to within 10% one need only measure V_F and scale:

$$E_K = \left(\frac{m_+}{m_e}\right) \quad V_F \left(1.09 \begin{matrix} + .1 \\ - 0. \end{matrix}\right) \quad . \tag{A2.6}$$

All probe theory analysis can do is to reduce the error bar below 10%, which in many cases is unnecessary. Compare (A2.6) with (4.4.4).

APPENDIX 3. ELECTRON MAGNETIC INSULATION

An electron is prevented from crossing a gap d across which it sees an accelerating potential E_{Ke} when a transverse magnetic field of B_c or larger is applied. The electron gyroradius is (see (6.2.1):

$$r_{ce} = \left(\frac{c}{\frac{eB}{m_{e0}}}\right)\sqrt{\left(\frac{E_{Ke}}{E_{0e}} + 1\right)^2 - 1} \qquad \text{(A3.1)}$$

Therefore, B_c is:

$$B_c = \frac{c}{\left(e/m_{e0}\right) d}\sqrt{\left(\frac{E_{Ke}}{E_{0c}} + 1\right)^2 - 1} \qquad \text{(A3.2)}$$

This can be recast as:

$$B_c = \frac{1}{c}\sqrt{\left(\frac{2E_{0e}\ E_{Ke}}{e^2\ d^2}\right)\quad\left(1 + \frac{E_{Ke}}{2\ E_{0e}}\right)} \qquad \text{(A3.3)}$$

where

$E_{0e} = m_{e0}c^2$ rest mass energy of the electron

c = speed of light.

APPENDIX 4. COMMENTS BY S. HUMPHRIES, JR.

The following comments are excerpted from a letter by Stanley Humphries, Jr. of Sept. 8, 1982.

On beam neutralization:

If electrons are totally confined, it is true that ions will be turned in a distance scale h(DL). On the other hand, in neutralized beams the maximum potential that can occur is of the order of (me/mi)Ei. When this potential is used in the effective Debye length, it gives an estimate of distances over which charge imbalance can occur. This quantity, h(E), is a factor of the square root of (mi/me) smaller than h(DL). I would consider that this length represents the dividing line between neutralized and unneutralized beams (as in Equations 2.4b and c). This is also the sheath width that appears in our calculations of longitudinal auto-neutralization (your equation 3.1.1). Although Fig. 2 is correct for protons, it might be better to recast the abscissa in terms of x/h(E), since the electron dynamics depends only on the ion velocity, not the mass of the ions.

On the transient probe response:

My interpretation of the floating probe differs somewhat from yours. The main differences from classical Langmuir probe theory are that the plasma is flowing with a velocity greater than the thermal velocities of ions and electrons and that the probe can act as a source of electrons (through secondary emission). Initially, the probe is at ground potential while the beam is at a positive potential. Ions impinge ballistically on the probe

while electrons are repelled, so the flux of fast ions is equal to or greater than that of neutralizing electrons. At the same time, electrons produced on the probe are attracted into the positive potential beam. These electrons can leave the probe until the probe reaches approximately the potential of the beam. The combination of ion collection and electron loss brings the probe close to Vs. More detailed calculations would be useful, but my guess is that such a probe will provide a direct measurement of Vs. In using an electrostatic probe, I would suggest a re-entrant construction such that the collector shields part of the insulator from direct beam bombardment to guard against insulator breakdown.

APPENDIX 5. COMMENTS BY T. R. LOCKNER

The following comments are excepted from a letter by T. R. Lockner of Sept. 17, 1982.

On the interpretation of floating probe response:

There are two assumptions in your discussion of floating probes which could lead to significant errors when interpreting the probe results. First, on Page 22, you assume that Vs = uEk. This is not necessarily true. The electron temperature will be a function of things such as the beam risetime, geometry of neutralization, and magnetic field geometry (possible self-magnetic fields). The fringing fields at the beam entrance will alter the electron temperature as will any oscillations in the electron sheath. If the beam electrons do not thermalize rapidly, the electron energy can rise to 4 uEk and the electron distribution function will be very non-Maxwellian. In addition, if the neutralization is not strictly longitudinal (the probe is also a source of electrons), the electron temperature and plasma potential will not agree with the theory you rely on. Because of temporal and 3-D effects, it will be very difficult to determine a priori what the electron temperature is.

On magnetic spectrometers:

There are many ways to attenuate an intense ion beam. The easiest is to drift the beam far enough so that the divergence drops the current density to a reasonable level. The beam could also be defocused at the source to

increase the divergence. If the beam is apertured, then drifted some distance, the current density will drop by $(d/r\theta)^2$, where $r\theta$ is the drift distance. Using a 2 mm aperture and drifting 1 meter, a beam with divergence of 2 degrees will drop in current density by a factor of 1000. The field coils can be electromagnetic with high mu pole pieces, thus reducing the size and weight.